ACS APPLIED ENERGY MATERIALS

www.acsaem.org Article

Thermomechanically Robust Ceramic/Polymer Nanocomposites Modified with Ionic Liquid for Hybrid Polymer Electrolyte Applications

Antonio del Bosque,* Bianca K. Muñoz, María Sánchez, and Alejandro Ureña

Cite This: ACS Appl. Energy Mater. 2022, 5, 4247−4258 Read Online

ACCESS | Metrics & More | Article Recommendations | Supporting Information

ABSTRACT: The development of hybrid electrolytes (HEs) that allows high mechanical properties and high ionic conductivity is a key in the smart mobility progress. In this article, various solid polymer electrolytes (SPEs) based on a blend of epoxy resins, ionic liquid, and titania or alumina nanoparticles have been manufactured and their electrochemical and thermomechanical performances have been evaluated. The combination of SPE components providing the highest properties was studied, having a significant influence on the type of nanoparticles and their dispersion. The electrolyte with the best combination of properties was L65P35(ILE)Al2, which showed T_g = 83 °C and E' at 30 °C = 1.2 GPa as thermomechanical properties, and $\sigma_0 = 7 \times 10^{-4}$ S/cm, $\sigma_1 = 1.6 \times 10^{-6}$ S/cm, and $C_{sp} = 5.6 \times 10^{-5}$ F/g at room temperature, as electrochemical properties. Moreover, the optimized electrolyte followed the Arrhenius ion transport model (E_a = 24.7 kJ/mol). These results would be promising for use as hybrid electrolyte in structural applications.

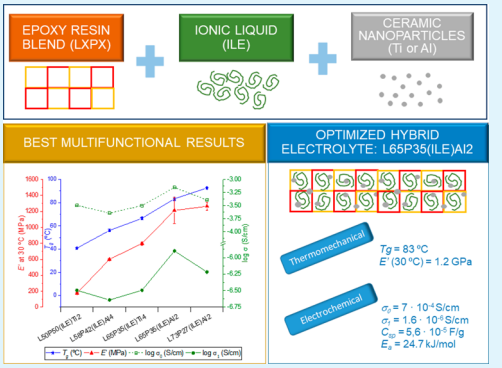

KEYWORDS: *polymer nanocomposite, epoxy-based resins, ionic liquid, structural composites, hybrid polymer electrolytes*

INTRODUCTION

Nowadays, there is an increasing worry about sustainability and energy demand in cities.[1] Therefore, all public administrations are making a great effort to boost the concept of smart mobility, which is a revolutionary form of transport that is cleaner, safer, and more efficient. In this scenario, one of the main objectives is electrification of vehicles, where the use of multifunctional supercapacitors and batteries based on composite materials is proposed that would fulfill the structural (mechanical and weight reduction) and energy storage functions.[2−4] However, these devices are not sufficiently developed to be incorporated into electric vehicles efficiently. To make this possible, in the future, the combination of these batteries and supercapacitors should be able to achieve the desired operation of the vehicles that integrate smart mobility. Possibly, the most complex challenge of these devices is to design solid polymers electrolytes (SPEs) that allow high mechanical properties and high ionic conductivity. The main drawback of SPEs is that these two properties are often in conflict and electrolytes with high mechanical properties have low ionic conductivity and vice versa.[2,5,6]

There are many different types of SPEs according to their components. Hybrid electrolytes (HEs) are electrolytes with more than two components that can be an alternative to traditional electrolytes to improve the ionic conductivity and mechanical strength of SPEs simultaneously.[7,8] HEs are classified into actives and passives electrolytes, depending on the nature of its fillers. For example, electrolytes with lithium-ion ceramic fillers such as Li_3N or $LiNbO_3$ are active and electrolytes based on ceramics fillers such us SiO_2 or TiO_2 are passive.[9] On the one hand, it is known that active HEs can afford better ion conduction than passive HEs because an extra ion conduction pathway exists through the fillers.[10] On the other hand, there is currently a growing interest in developing passive HEs because they have a higher mechanical and thermal stability than active HEs,[9] being substantially less expensive. Passive HEs with ceramic fillers such as SiO_2, TiO_2, Al_2O_3, ZrO_2, ZnO, and clays have shown promising performance properties for structural applications. It was suggested that the presence of inorganic species at the interface with the polymer chains generates a grain boundary effect, which significantly increases the ionic conductivity observed.[11] Also, Lewis acid/base interactions between the surface groups of ceramic nanoparticles, ionic species (lithium salt or ionic liquids), and polymeric segments facilitate ion dissociation and

Received: December 6, 2021
Accepted: March 15, 2022
Published: March 29, 2022

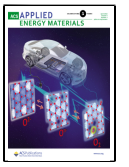

https://doi.org/10.1021/acsaem.1c03836
ACS Appl. Energy Mater. 2022, 5, 4247−4258

possibly create preferential conduction pathways at the limits of ceramic nanoparticles.[12,13]

There is a great effort in developing silica-based HEs. Yuuki et al. used surface amino-functionalized silica nanofibers (average diameters = 400 and 1000 nm) as one-dimensional (1-D) fillers with ionic liquid in lithium salt. They noticed that the well-dispersed 1-D nanofillers easily form a three-dimensional network structure in the ionic liquid, act as physical cross-linkers, and increase the viscosity of the composites, providing a quasi-solid state with a high ionic conductivity.[14] Chaurasia and Chandra manufactured HEs based on silica and a PEO matrix containing different amounts of lithium salt with a good mechanical stability. In this case, the ionic conductivity increased with increasing concentrations of lithium salt, reaching a value of 1.24×10^{-6} S/cm at 30 °C (1.15×10^{-4} S/cm at 100 °C) for a 20 wt % lithium salt load in the matrix.[15] Feng et al. studied structural electrolytes based on polyethylene glycol (PEG-600 and PEG-2000), epoxy resin, and nanosilica, together with LiTFSI dissolved in ethylene glycol. The more content in nanoparticles increased the ionic conductivity, but mechanical properties decreased. The best electrolyte achieved an ionic conductivity of 8.6×10^{-5} S/cm, a T_g of 43 °C, and an elastic modulus of 135 MPa.[16] Khurana et al. reported the properties of HE films incorporating different amounts of surface modified SiO_2 nanoparticles and electrolyte solution (lithium salt in ionic liquid) in poly(vinylidene fluoride hexafluoropropylene) (PVdF-HFP). The effect of a better dispersion of the modified nanoparticles in the polymer matrix was reflected by the enhancement of the ionic conductivity of electrolytes with modified SiO_2 ($\sim 2.94 \times 10^{-3}$ S/cm) compared to the ones with no SiO_2 and unmodified SiO_2 ($\sim 1.90 \times 10^{-3}$ S/cm and $\sim 1.56 \times 10^{-3}$ S/cm, respectively). However, these electrolytes showed low mechanical properties, for example, tensile strength obtained for electrolytes with modified SiO_2 (1.8 MPa) is higher in comparison with unmodified SiO_2 (1.2 MPa) and without SiO_2 (0.55 MPa).[17]

Titania is used as another promising filler for the development of passive HEs. Chen et al. designed and prepared a rigid−flexible HE based on PVdF-HFP, TiO_2 rigid framework, and ionic liquid. This HE exhibited high ionic conductivity (7.4×10^{-3} S/cm at 25 °C), electrochemical stability, and a mechanical flexibility tunable by adjusting the ratio of PVdF-HFP and TiO_2.[18] Pignanelli et al. reported a synergistic in situ synthesis of lithium-ion poly(ethylene citrate) with embedded titania nanoparticles in which the esterification process itself triggered the hydrolysis of the titanium alkoxide precursor to form a promising fluorine-free lithium-ion solid polymer electrolyte. With this system a slight increase in the degree of polymerization and thermal stability for HE observed by increasing titania nanoparticles concentration. In consequence, a two-order magnitude increase in the ionic conductivity was observed, yielding 1.74×10^{-4} S/cm for a 20% weight fraction of titania nanoparticles.[19] Li et al. manufactured structural electrolytes based on poly(ethylene glycol) diglycidyl ether (PEGDGE), mesoporous TiO_2 nanoparticles (until 10 wt %), and tetrabutylammonium hexafluorophosphate salt dissolved in PC, as electrolyte. This work concluded that the hydroxyl groups attached to the TiO_2 promote the cross-linking reaction of the resin, which positively affects the mechanical and electrochemical performance of the HE. The highest ionic conductivity (11×10^{-5} S/cm) and compression strength (5.06 MPa) were obtained for a HE with 6 wt % TiO_2.[20] In a recent study, we have developed a HE based on blend epoxy resins with PEGDGE, and a commercial epoxy resin (Araldite LY556) based on diglycidyl ether of bisphenol A (DGEBA), using the suggested commercial hardener Araldite XB3473 and 4,4-diphenylsulfonylmethane. The additives included the obtained ionic conductivity and were ionic liquid and titania nanoparticles. Our optimized HE showed promising mechanical properties (T_g > 70 °C and storage modulus at 30 °C > 1 GPa), and it was used in a proof of concept for a supercapacitor made of graphene coated woven carbon fibers.[5,21]

HEs reinforced with alumina particles have also shown an improvement of the electrochemical and mechanical properties. Croce et al. were pioneers using alumina nanoparticles in solid electrolytes. In their study, three types of Al_2O_3 nanoparticles with acidic, neutral, and basic surface characteristics were incorporated in $P(EO)_{20}LiSO_3CF_3$. This study reveals that SPE with acidic and neutral alumina shows a greater degree of improvement in conductivity over SPE with basic alumina, which led the authors to propose that the predominant mechanism in conductivity is specific Lewis acid interactions.[22] In further studies reported by Jayathilaka et al. with $P(EO)_9LiTFSI/Al_2O_3$, this effect was not remarkable[23] and in other cases, Marcinek et al. observed that the addition of Al_2O_3 in PEG−$LiClO_4$ resulted in an increase in ionic conductivity in the narrow lithium salt concentration range.[24] Best et al. observed a decrease in conductivity with the addition of TiO_2 or Al_2O_3 nanoparticles in the electrolyte based on polyether and poly(methylene ethylene oxide). At this point, there was not a clear trend in ionic conductivity variation with the type of surface functional group of the nanoparticles and it was suggested that the specific interactions depend on the type of anions and the polymer matrix used.[25] In recent studies, Singh and Rafiuddin developed a HE based on polyaniline as a matrix and silver phosphate using alumina as filler at different compositions having the formula $(1 - x)PANI\text{-}Ag_3PO_4 \cdot xAl_2O_3$ with x ranging from 0.0 to 0.6. The conductivities recorded over a temperature range of 40−250 °C were in the range of 10^{-3} to 10^{-5} S/cm, where the maximum ionic conductivity was seen in the composition x = 0.2 at 240 °C.[26] Kumar and Rao developed a nanocomposite polymer by doping sodium acetate (CH_3COONa) into poly(vinylpyrrolidone) (PVP) and dispersing alumina through the solution cast method. The highest ionic conductivity was found to be 1.05×10^{-3} S/cm for the prepared film with weight percent ratio of PVP + CH_3COONa:Al_2O_3 (80:20:1 (%)).[27] Pradeepa et al. made a composite with poly(vinyl alcohol) (PVA) and poly(methyl methacrylate) blend using different contents of alumina filler, to examine the filler addition effect on the structural and electrochemical properties. From the ionic conductivity results, the HE with 4 wt % alumina filler showed the highest ionic conductivity (8.76×10^{-3} S/cm) with an excellent thermal stability at room temperature.[28] Kwon et al. made an epoxy HE with ionic liquid, lithium salt, and alumina nanowires that showed an excellent stiffness ($E \approx 1$ GPa at 25 °C) and good conductivity (2.9×10^{-4} S/cm at 25 °C).[29] Although many questions remain to be answered about the use of passive ceramics in solid electrolytes, ceramic reinforcements are currently being used as additives to improve SPE properties.

As has been deduced from the state-of-the-art, it seems evident that any change in the composition of HEs can affect the cross-linking mechanism and completely modify their

https://doi.org/10.1021/acsaem.1c03836
ACS Appl. Energy Mater. 2022, 5, 4247−4258

electrochemical, thermal, and mechanical behavior. Thus, the ideal multifunctional HE for structural applications would reach the elastic modulus and T_g of an aeronautical epoxy resin (around 2.65 GPa and 150 °C, respectively), and the ionic conductivity of an ionic liquid (around 10^{-2} S/cm). Nowadays, there is not an electrolyte that maintains all of these properties. So, much effort must be focused to achieve a HE with properties close to the ideal multifunctional. In this study, a series of polymer nanocomposites based on a blend of DGEBA/PEGDGE epoxy resins with ionic liquid and titania or alumina nanoparticles have been developed with the aim of finding nanocomposites that act as HE in structural applications. The effect of their composition on the ionic conductivity, thermomechanical properties, and microstructure has been discussed. In this work, one of the manufactured passive hybrid electrolytes achieves a relationship between ionic conductivity and structural properties that is closer to the ideal multifunctional electrolyte than those developed in the state-of-the-art; especially, it shows thermomechanically robust behavior.

METHODS

Materials. HEs are based on a mixture of epoxy resins, ionic liquid, and ceramic nanoparticles. The first epoxy resin was based on diglycidyl ether of bisphenol A, obtained from a commercial monomer (Araldite LY556) cured with a commercial mixture of amines (Araldite XB3473) in a weight ratio of 100:23 between these components, respectively. This resin is a viscous liquid (5200−6000 mPa·s at room temperature) with application in aeronautical structural composites, supplied by HUNTSMAN. The epoxy resin LY556/XB3473 will be called L. The second epoxy resin used was poly(ethylene glycol) diglycidyl ether (PEGDGE), which has a viscosity of 60−110 mPa·s at room temperature and a molecular weight of 500 g·mol^{-1}; therefore, it contains 9−10 ethylene oxide units approximately, supplied by MERCK. The hardener was a 4,4′-diaminodiphenylsulfone (DDS), which is an amino hardener with a 99% purity, supplied also by MERK. PEGDGE/DDS were used in the weight ratio of 100:35, respectively, and it will be called P. Moreover, ionic liquid was 1-ethyl-3-methyl-imidazolium bis-(trifluoromethylsulfonyl)imide (ILE) and it had a 99% purity, supplied by IOLITEC; titania nanoparticles (TiO_2) had a maximum size of 25 nm with 99.7% purity and alumina nanoparticles (Al_2O_3) had a maximum size of 13 nm with 99.8% purity. They were used as received and were supplied by MERCK.

Manufacturing of HEs. The composition of all of the samples prepared and their nomenclature are listed in Table 1. As a common matrix, the samples contain a variable mixture of the resin system L/P (LY556/XB3473 (L) and PEGDGE/DDS (P), L/P ratio = 1), 30 wt % of ionic liquid (ILE), and either alumina (Al) or titania (Ti) nanoparticles (2−8 wt %) by adjusting the matrix contents. The nanoparticles content was calculated on the basis of L/P + ILE. Furthermore, other electrolytes manufactured in the same way in a previous work will be also used to discuss the results.[5]

Electrolytes were manufactured in two different ways depending on their composition. On the one hand, electrolytes based on epoxy resins and ionic liquid were manufactured as follows: a mixture of epoxy monomers (Araldite L556 and PEGDGE) and ionic liquid (ILE) was degasified under vacuum conditions in a magnetic mixer during 45 min at 40 °C, in order to homogenize the mixture and properly remove the entrapped air. Then, the hardeners (Araldite XB3473 and DDS) were added and mixed at 40 °C. Lastly, the mixture was poured on a metallic open mold previously smeared with release agent and cured at 140 °C for 8 h in an oven.

On the other hand, electrolytes based on epoxy resins, ionic liquid, and ceramic nanoparticles were manufactured following the above procedure, but the nanoparticles were added before the hardeners and after homogenization process. The nanoparticles were dispersed in the mixture by ultrasonication in a Hielscher ultrasonic processor UP400 St at 0.5 pulse cycles and 50% amplitude. This technique induces the breakage of nanoparticles' agglomerates due to the cavitation forces induced by the ultrasonic pulses. Here, 1 h of this process was enough to guarantee a good nanoparticle dispersion, as reported in other systems based on epoxy resins with ceramic nanoparticles with a similar size.[21,30,31] In this case, a rotary mold made of aluminum was used during curing cycle to avoid the nanoparticles sedimentation. With this mold, samples with 150 × 65 × 15 mm^3 dimensions were manufactured in order to cut the specimens with the desired geometry for their subsequent characterizations.

Table 1. Composition of Epoxy Systems Based on L and P as Matrix[a]

	wt %			
sample	L	P	ILE	TiO_2/Al_2O_3
L80P20(ILE)Ti4	52.8	13.2	30	4.0
L80P20(ILE)Al2	54.4	13.6	30	2.0
L80P20(ILE)Al4	52.8	13.2	30	4.0
L73P27(ILE)Ti4	48.2	17.8	30	4.0
L73P27(ILE)Al2	49.6	18.4	30	2.0
L73P27(ILE)Al4	48.2	17.8	30	4.0
L65P35(ILE)Ti4	42.9	23.1	30	4.0
L65P35(ILE)Ti6	41.6	22.4	30	6.0
L65P35(ILE)Ti8	40.3	21.7	30	8.0
L65P35(ILE)Al2	44.2	23.8	30	2.0
L65P35(ILE)Al4	42.9	23.1	30	4.0
L65P35(ILE)Al6	41.6	22.4	30	6.0
L58P42	58	42		
L58P42(ILE)	40.6	29.4	30	
L58P42(ILE)Ti2	39.4	28.6	30	2.0
L58P42(ILE)Ti4	38.3	27.7	30	4.0
L58P42(ILE)Ti6	37.1	26.9	30	6.0
L58P42(ILE)Ti8	36	26	30	8.0
L58P42(ILE)Al2	39.4	28.6	30	2.0
L58P42(ILE)Al4	38.3	27.7	30	4.0
L58P42(ILE)Al6	37.1	26.9	30	6.0
L50P50(ILE)Ti4	33	33	30	4.0
L50P50(ILE)Al2	34	34	30	2.0
L50P50(ILE)Al4	33	33	30	4.0

[a]L = LY556/XB3473 (100:23), P = PEGDGE/DDS (100:35), ILE = 1-ethyl-3-methyl-imidazolium bis(trifluoromethylsulfonyl)imide.

Thermomechanical Characterization. The thermomechanical properties were studied with Dynamic mechanical thermal analysis (DMTA) method, following the ASTM 5418 in a DMTA Q800 (TA Instruments) machine. Three samples with dimensions of 17.5 × 12 × 1.25 mm^3 of each condition were tested in a single cantilever mode over a temperature range from 20 to 200 °C, using a frequency of 1 Hz and a heating rate of 2 °C/min. The glass transition temperature (T_g) was measured as the maximum of the loss tangent curve (tan δ). In addition, the storage modulus (E') was determined at 30 °C, with the aim of evaluating and comparing the stiffness of the samples.

Electrochemical Characterization. The electrochemical properties were evaluated using an AUTOLAB PGSTAT302N potentiostat. For these experiments, three samples with 30 × 20 × 2 mm^3 dimensions were dried in a vacuum oven at 80 °C for 4 h and, later, they were analyzed in an adjustable electrochemical cell. In this cell, HE was located between two symmetric polished and clean stainless-steel electrodes with the same sample dimensions (30 × 20 mm^2). Moreover, this electrochemical cell contained mechanical joints that were able to exert pressure over the electrodes to promote electrode/electrolyte contact. The electrochemical cell is shown in Figure 1.

https://doi.org/10.1021/acsaem.1c03836
ACS Appl. Energy Mater. 2022, 5, 4247−4258

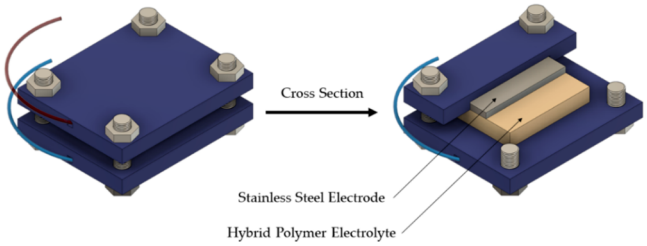

Figure 1. Electrochemical cell design.

Electrochemical Impedance Spectroscopy. The electrochemical impedance spectroscopy (EIS) response was measured at room temperature for all HEs manufactured and between room temperature and 120 °C for the HEs with the best properties with and without nanoparticles. AC impedance was measured using an initial frequency of 1 MHz and a final frequency of 0.1 Hz and an amplitude of 30 mV. The Nyquist plots presented a semicircle at high frequencies and another semicircular contribution at lower frequencies corresponding to R_0 (R_1CPE$_1$) (R_2CPE$_2$) equivalent circuit, where each part of the circuit simulates certain areas of the Nyquist diagram, indicated in Figure 2 with different colors. Each sample was subjected to three consecutive measurements.

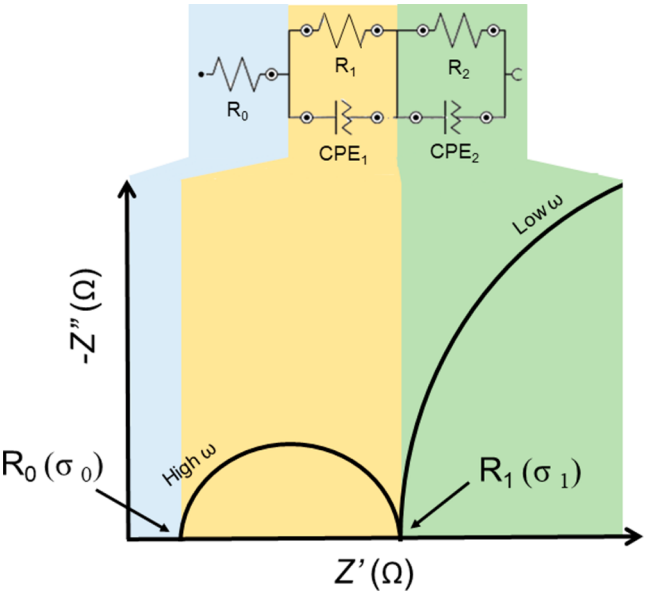

Figure 2. Characteristic Nyquist diagram and equivalent circuit of these HEs.

In these types of electrolytes, the ionic conductivity in S/cm was calculated using eq 1:

$$\sigma = \frac{t}{RA} \quad (1)$$

where t is the thickness of the HEs in cm (between 0.20 and 0.25 cm), A is the area of the sample in cm^2 (6.0 cm^2), and R was obtained from the X-intercept of the high-frequency region in the Nyquist plot as previously reported.[5] Two conductivity values were calculated using R_0 and R_1 (marked as σ_0 and σ_1) and correspond to the interface and bulk contributions, respectively.[5]

Linear Sweep Voltammetry. The electrochemical stability of the HEs with better properties with and without nanoparticles was studied using linear sweep voltammetry (LSV) on the stainless-steel/HE/stainless-steel cell at a constant rate of 0.1 V/s from −4 to 4 V at room temperature.

Cyclic Voltammetry. Cyclic voltammetry (CV) tests were carried out in order to determine the specific capacitance of the stainless-steel/HE/stainless-steel cell with better properties with and without nanoparticles. The electrochemical response was recorded in a voltage window of −1 to 1 V at a voltage scan rate of 0.1 V/s. Each sample was subjected to five consecutive voltammetry cycles.

Microstructural Characterization. Cryofractured surfaces were morphologically analyzed using field-emission gun scanning electron microscopy (FEG-SEM) Nova NanoSEM 230 apparatus. First, ILE was extracted by introducing the samples in ethanol for 1 week, changing the solvent twice a day, and drying the samples in a vacuum oven at 70 °C overnight. Cryofractured samples were studied after coating with a gold sputtering (5−7 nm Au).

Cross-Polarization Magic Angle Spinning Nuclear Magnetic Resonance. The sample L65P35(ILE)Al2 was analyzed at room temperature on a Bruker Advanced III 400 spectrometer HD-WB (operating at a magnetic field of 9.4 T), with a maximum spinning frequency to 25 kHz. Frequencies are given for ^{13}C (100.13 MHz), ^{19}F (376.5 MHz), and ^{27}Al (104.2 MHz). ^{27}Al, ^{13}C, and ^{19}F chemical shifts were referenced to $Al(NO_3)_3$ in D_2O, TMS, and $CFCl_3$, respectively. The sample was milled using a grinder and directly weighted in the 4 mm probe (75−100 mg of sample).

RESULTS AND DISCUSSION

Dynamic Thermomechanical Characterization. In order to stablish an ideal formulation that achieves the best relationship between thermomechanical and electrochemical properties in HEs, samples containing either alumina or titania in different proportions (2−8 wt %) were fabricated using different L/P ratios 80/20, 73/27, 65/35, 58/42, and 50/50 and keeping a 30 wt % amount of ionic liquid (ILE). All of the samples were characterized by DMTA in order to evaluate their thermal stability and their mechanical potential for structural applications. T_g, E' at 30 °C, and E'' of the samples are listed in Table 2.

For comparison, the results obtained in a previous study for the neat resin samples containing different L/P resin ratios and 30 wt % ILE are shown. It has been previously observed that the composition of the epoxy resin blends had influence directly on the mechanical resistance of the samples, making them suitable for SPE applications.[5,16] For the neat resin samples, LP, and the mixtures modified with ionic liquid, LP(ILE), T_g and E' at 30 °C followed a linear behavior depending on the content of L or P resin, from the higher values with the greater content of L to the lower values with the greater content of P (T_g of pristine L and P resins are 161 and 9 °C, respectively).[5] When the nanoparticles were included, this linearity was no longer observed, but it kept the tendency decreasing of T_g and E' at 30 °C when the amount of P resin increased. This drop can be explained by the elastomeric behavior shown by resin P at room temperature due to the presence of ethylene glycol units in its structure. Figure 3 shows T_g vs the LP(ILE)NPs with different LP content for the samples modified with 2 and 4 wt % titania (Ti) and alumina (Al) NPs. When titania nanoparticles were included (Figure 3) the maximum T_g was obtained for the L80P20(ILE)Ti2 and L80P20(ILE)Ti4, but as soon as the amount of P resin increased, the T_g droped drastically (more than 40 °C) by including only a 7 wt % greater amount of P resin to the blend (L73P27(ILE)Ti2 and -4 ratio). Then, by decreasing the amount of L resin, T_g decreased but not as abruptly as that observed in the previous case. When alumina nanoparticles were included (Figure 3), there were not remarkable differences between the T_g for the samples containing L80P20 and L73P27 ratios. Furthermore, from L65P35 to L50P50 the linear decrease was recovered.

https://doi.org/10.1021/acsaem.1c03836
ACS Appl. Energy Mater. 2022, 5, 4247−4258

Table 2. Thermomechanical Properties and Ionic Conductivities of Different HEs[a]

		DMTA			ionic conductivity		
entry	sample	T_g (°C)	E' at 30 °C (MPa)	E'' (MPa)[b]	σ_0 (S/cm)	σ_1 (S/cm)	ref
1	L80P20	131 ± 2	2867 ± 32	249 ± 10			5
2	L80P20(ILE)	120.1 ± 0.9	1762 ± 29	107 ± 3		2.0×10^{-8}	5
3	L80P20(ILE)Ti2	111.3 ± 0.3	1983 ± 8	132 ± 1			5
4	L80P20(ILE)Ti4	110.5 ± 0.4	1988 ± 19	135 ± 6			this study
5	L80P20(ILE)Al2	90.8 ± 0.1	1695 ± 55	127 ± 10		1.8×10^{-7}	this study
6	L80P20(ILE)Al4	87.7 ± 0.1	1634 ± 14	134 ± 1		1.3×10^{-8}	this study
7	L73P27	116 ± 1	2733 ± 92	239 ± 21			5
8	L73P27(ILE)	87.9 ± 0.6	1359 ± 141	100 ± 9		4.3×10^{-8}	5
9	L73P27(ILE)Ti2	77.0 ± 0.4	1157 ± 48	112 ± 5		2.0×10^{-7}	5
10	L73P27(ILE)Ti4	65 ± 1	786 ± 28			2.1×10^{-8}	this study
11	L73P27(ILE)Al2	92.5 ± 0.8	1263 ± 52	101 ± 3	4.0×10^{-4}	6.1×10^{-7}	this study
12	L73P27(ILE)Al4	91.8 ± 0.8	1667 ± 76	132 ± 5		1.4×10^{-7}	this study
13	L65P35	102 ± 1	2536 ± 176	276 ± 18			5
14	L65P35(ILE)	65.4 ± 0.2	841 ± 21			1.3×10^{-7}	5
15	L65P35(ILE)Ti2	70 ± 2	1154 ± 97			2.1×10^{-7}	5
16	L65P35(ILE)Ti4	67 ± 1	797 ± 182		3.1×10^{-4}	3.2×10^{-7}	this study
17	L65P35(ILE)Ti6	62 ± 1	944 ± 77			1.1×10^{-7}	this study
18	L35P35(ILE)Ti8	60 ± 1	597 ± 38			4.6×10^{-8}	this study
19	L65P35(ILE)Al2	83 ± 1	1213 ± 164	93 ± 1	7×10^{-4}	1.6×10^{-6}	this study
20	L65P35(ILE)Al4	71 ± 1	902 ± 32			1.6×10^{-7}	this study
21	L65P35(ILE)Al6	70.1 ± 0.1	857 ± 46			7.2×10^{-8}	this study
22	L58P42	86.9 ± 0.3	2216 ± 49	206 ± 6			this study
23	L58P42(ILE)	50.2 ± 0.1	381 ± 6			1.8×10^{-7}	this study
24	L58P42(ILE)Ti2	54.2 ± 2	410 ± 35			2.1×10^{-7}	this study
25	L58P42(ILE)Ti4	52 ± 1	406 ± 21			1.1×10^{-7}	this study
26	L58P42(ILE)Ti6	50 ± 2	330 ± 29			7.1×10^{-7}	this study
27	L58P42(ILE)Ti8	51.3 ± 0.1	288 ± 8			3.8×10^{-8}	this study
28	L58P42(ILE)Al2	54 ± 1	476 ± 21			1.9×10^{-7}	this study
29	L58P42(ILE)Al4	56 ± 1	598 ± 8		2.3×10^{-4}	2.3×10^{-7}	this study
30	L58P42(ILE)Al6	54 ± 3	354.9 ± 0.5			8.3×10^{-8}	this study
31	L50P50	72.7 ± 0.3	2850 ± 20	251 ± 20			5
32	L50P50(ILE)	48.9 ± 0.4	410 ± 20	212 ± 9	3.2×10^{-4}	1.9×10^{-8}	5
33	L50P50(ILE)Ti2	47 ± 3	450 ± 20	169 ± 7		3.2×10^{-7}	5
34	L50P50(ILE)Ti4	31 ± 4	95 ± 12			9.6×10^{-8}	this study
35	L50P50(ILE)Al2	40.1 ± 0.9	329 ± 0.8			9.5×10^{-8}	this study
36	L50P50(ILE)Al4	41.2 ± 0	142 ± 0			5.6×10^{-8}	this study

[a]L = LY556/XB3473 (100:23), P = PEGDGE/DDS (100:35), ILE = 1-ethyl-3-methy-imidazolium bis(trifluoromethylsulfonyl)imide, Ti = titania NPs, and Al = alumina NPs. [b]E'' values only for samples that reach the maximum peak of its curve for temperatures above 20 °C.

This effect could be explained due to a combination of the viscosity of the mixtures and the nanoparticle size, and, in addition, it can also be greatly influenced by the particle agglomeration, the solid load and the specific surface area. The L resin is a very viscous resin compared to P resin (5200−6000 mPa·s and 60−110 mPa·s, respectively). It was observed that the less viscous resins gave rise to a better dispersion of nanoparticles after the sonication. However, as soon as the viscosity decreased, if the nanoparticles were not well dispersed, they can sediment down to the bottom of the mold promoting a reduction of its properties. Moreover, the size of the nanoparticle also played an important role in the dispersion, since smaller nanoparticles (Al) can promote better dispersion than bigger ones (Ti) in these mixtures with sonication technique, due to a freer mobility of nanoparticles. In addition, the critical filler load decreases with increasing the fillers surface area.[32] If the small nanoparticles are well-dispersed and -stabilized, a viscous media will avoid their decantation. However, if the dispersion is not well-stabilized, the nanoparticles can be agglomerated, and the clusters formed could favor the decantation even using a rotary mold. This could explain why the samples containing alumina seemed to show higher T_g and storage modulus (Figure 4) for the same L/P ratio (Al_2O_3 (13 nm) vs TiO_2 (25 nm)). The smallest alumina nanoparticles gave rise to a better-stabilized and dispersed sample even at low viscosities. To confirm this, the microstructure of the samples was analyzed to compare the dispersion in the samples containing either alumina or titania nanoparticles.

Different magnifications of FEG-SEM images corresponding to the samples L65P35(ILE)NP2 containing 2 wt % titania or alumina are shown in Figure 5.

The cryofracture of the sample containing titania (L65P35-(ILE)Ti2) clearly showed the presence of nanoparticles clusters of 3 μm approximately (Figure 5a−c), while the sample containing alumina (L65P35(ILE)Al2) showed a well-dispersed nanocomposite where the nanoparticles were homogeneously distributed along a less fibrous surface (Figure 5d−f). Moreover, titania clusters observed in L65P35(ILE)Ti2 sample could act as stress concentration points and cracks

https://doi.org/10.1021/acsaem.1c03836
ACS Appl. Energy Mater. 2022, 5, 4247−4258

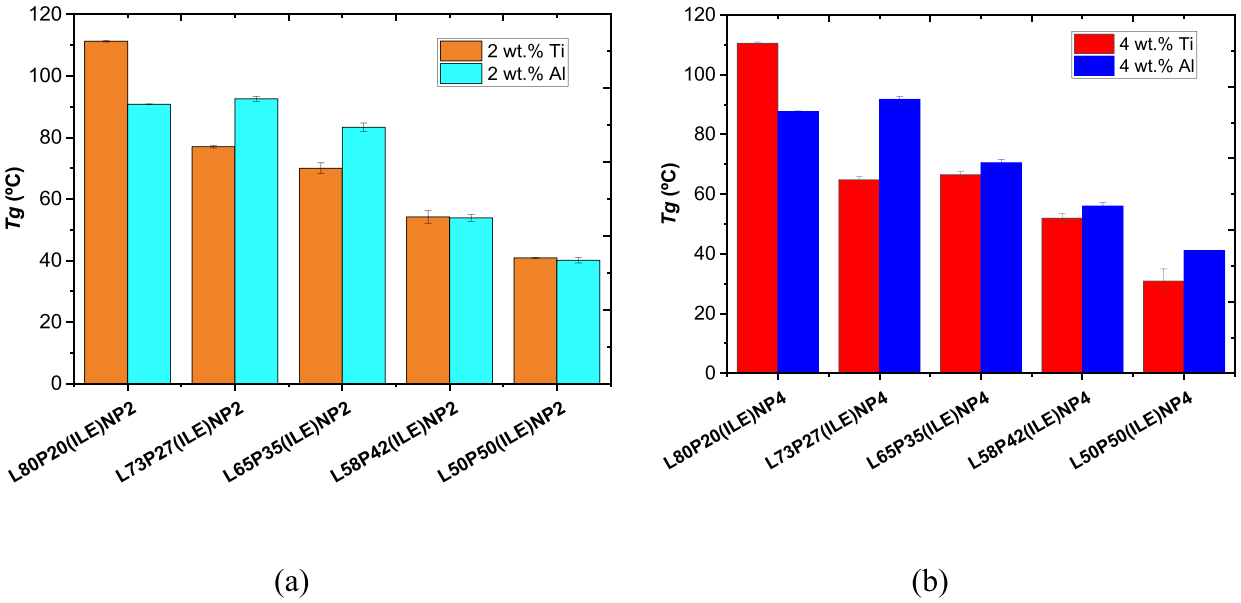

Figure 3. T_g values of the samples modified with (a) 2 and (b) 4 wt % titania or alumina nanoparticles.

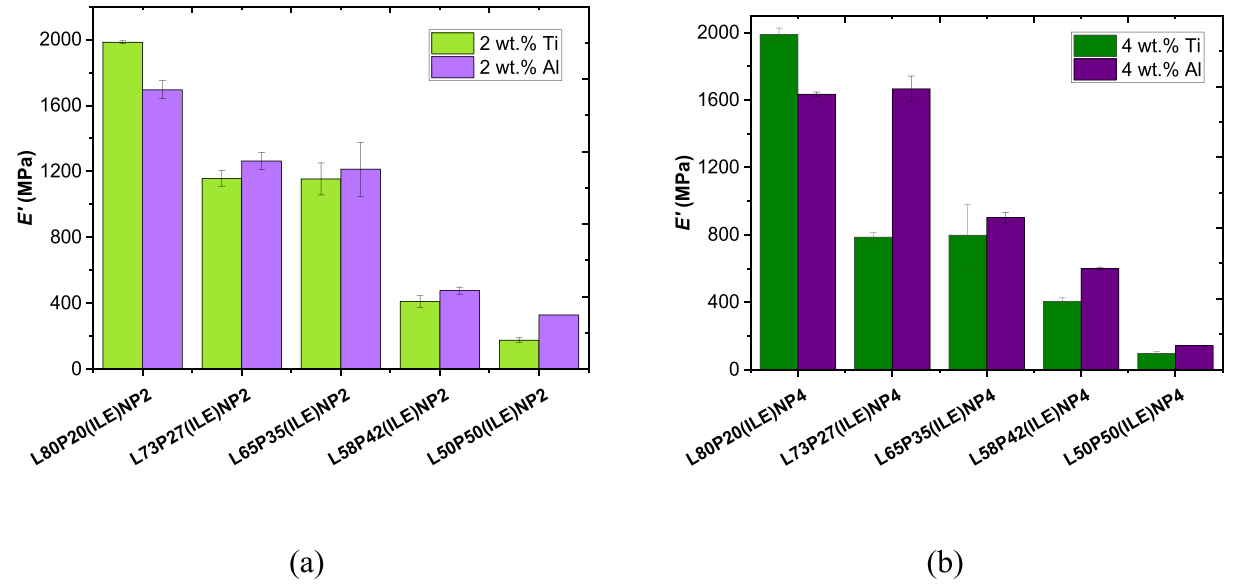

Figure 4. E' at 30 °C of the samples modified with (a) 2 and (b) 4 wt % titania or alumina nanoparticles.

appeared through the nanoparticles. Conversely, L65P35-(ILE)Al2 sample had a rougher structure at higher magnification (Figure 5f), which indicated that the crack individually interacted with the alumina nanoparticles. The good dispersion of alumina nanoparticles improved the polymerization producing a higher cross-linked polymer with a better interfacial interaction between the reinforcement and the matrix,[29,31] except for L80P20 electrolytes where the higher viscosity of the mixture (higher content of L) could promote a worse dispersion of the nanoparticles with more agglomerates. Thus, it could be explained why the T_g and the storage modulus were slightly higher for the samples containing alumina (T_g values 83 °C vs 70 °C, Table 1, entries 15 and 19), taking into account the commented exception.

Electrochemical Characterization. The different HEs were analyzed by EIS. The values needed to calculate the ionic conductivity according to R_0/σ_0 and R_1/σ_1 were extracted from the Nyquist plots and their fit to the equivalent circuit. The values of ionic conductivity are indicated in Table 2. The Nyquist plots and the equivalent circuit parameters for all of the samples are shown in Figures S1−S7 and Tables S1−S8 of the Supporting Information.

The ionic conductivity, σ_1, was calculated from the diameter of the high-frequency arc (R_1) and it is attributed to the bulk ion transport as it was previously reported. In some cases, it was possible to calculate the ionic conductivity from the high-frequency X-intercept semicircle at 1 MHz $(R_0)\sigma_0$, attributed to the contribution of the interfacial boundaries of titania or alumina and the electrolyte to provide fast ion transport across the current flow. The last ionic transport mode was not exhibited by all of the nanocomposites prepared in this study, since it seems to depend on an appropriate dispersion and percolation of the nanoparticles across the surface. On the

https://doi.org/10.1021/acsaem.1c03836
ACS Appl. Energy Mater. 2022, 5, 4247−4258

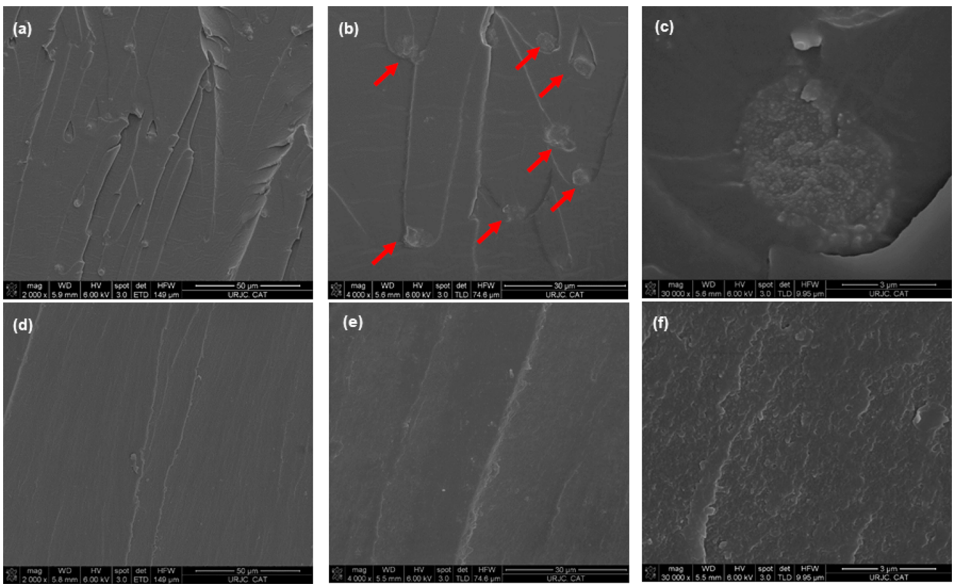

Figure 5. FEG-SEM images of the samples L65P35(ILE)NP2 modified with 2 wt % titania (a–c) or alumina nanoparticles (d–f). Scale bar: (a, d) 50 μm, (b, e) 30 μm, and (c,f) 3 μm.

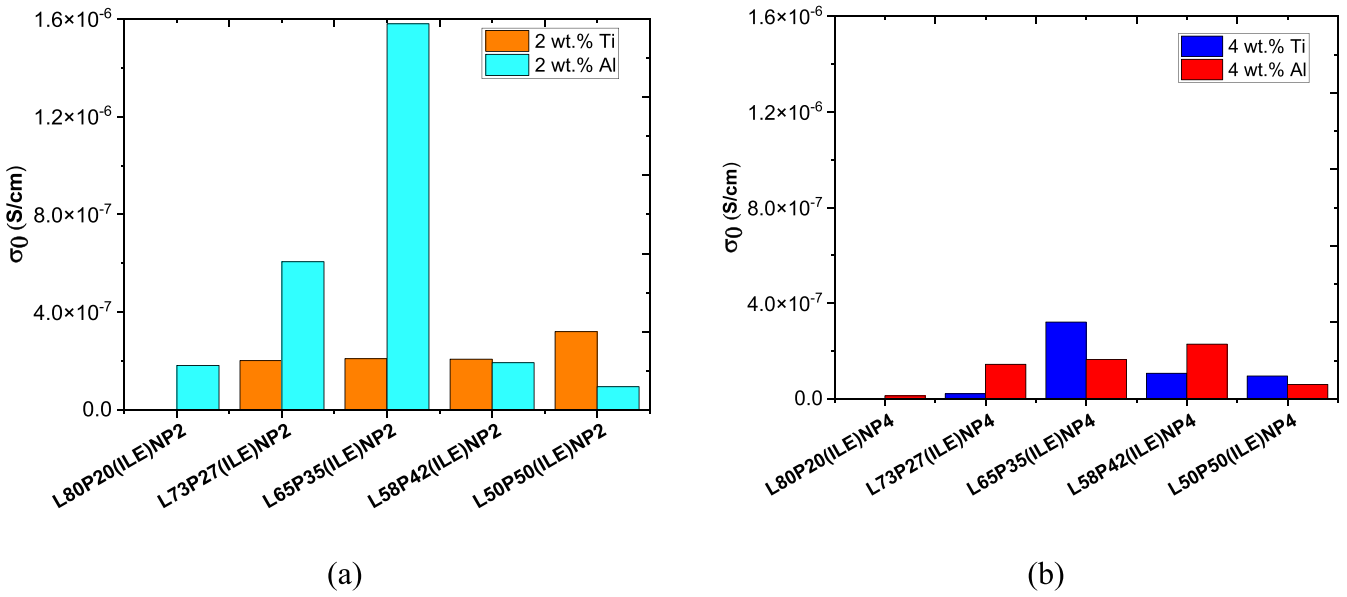

Figure 6. Ionic conductivities of the samples modified with (a) 2 and (b) 4 wt % titania or alumina nanoparticles.

basis of this, σ_0 was only calculated for samples that fit that model in the equivalent circuit (L50P50(ILE)Ti2, L65P35-(ILE)Ti4, L65P35(ILE)Al2, L73P27(ILE)Al2, and L58P42-(ILE)Al4), while σ_1 was calculated for all of the samples where the ion transport is more plausible to occur through the polymer bulk. As it was mentioned in the Introduction, getting high ionic conductivities in samples with high mechanical properties is a challenge since these two properties are usually in conflict. The ionic conductivity for the more rigid samples was usually very low ($<10^{-8}$ S/cm) or was not even possible to measure. The ionic conductivity of LP(ILE)NPs samples modified with 2 and 4 wt % titania (Ti) and alumina (Al) nanoparticles with different LP content are shown in Figure 6.

In general, at higher L content non-existent or very low ionic conductivity can be detected due to the rigidity of the samples, manifested in a low mobility of the polymer chains. Then, as the P resin content (more elastomeric resin) increase, the ionic conductivity seems to appear and increase up to a maximum value, but these samples do not correspond to the samples exhibiting the worst mechanical performance. Therefore, this fact indicates that the ionic conductivity in these nanocomposites not only depends on the stiffness or matrix cross-linked network but on a combination of several factors mainly governed by the nanoparticle dispersion in the composites.

In general, low percentages of nanoparticles promoted a higher value of ionic conductivity; in this case, electrolytes with 2 wt % nanoparticles usually reported higher conductivities than 4, 6, or 8 wt %. This could be because low percentages favored the adequate dispersion of the reinforcement and, thus, favored the correct interactions of the ethylene glycol units of the P with nanoparticles through the creation of cylindrical tunnels, which provided a pathway for the movement of cations.[33] When the particle content is increased to more than 2 wt %, the ionic conductivity drops. The higher content of

https://doi.org/10.1021/acsaem.1c03836
ACS Appl. Energy Mater. 2022, 5, 4247–4258

nanoparticles favored the appearance of large agglomerates that deteriorate the ionic conductivity values by obstructing these cylindrical tunnels that provide a pathway for ionic mobility.[16,29,33]

Particularly, the introduction of 2 wt % titania nanoparticles showed an increase of ionic conductivity when the P resin content increased reaching a maximum value for the sample L50P50(ILE)Ti2 (Figure 6a). When 4 wt % titania is used, the optimum ionic conductivity value was observed for the sample L65P35(ILE)Ti4 followed by detrimental values as the L content decreases (Figure 6b). For alumina, the introduction of 2 wt % led to achieving a maximum for L65P35(ILE)Al2 (Figure 6a), and with the introduction of 4 wt % the best sample seemed to be L58P42(ILE)Al4 (Figure 6b).

Selection of Optimal Electrolytes and Comparative with the State-of-the-Art. In order to select the electrolyte with the best combination of thermomechanical properties and ionic conductivity, characteristics of a multifunctional material, the DMTA data of the samples exhibiting the best ionic conductivities are represented in Figure 7. According to these

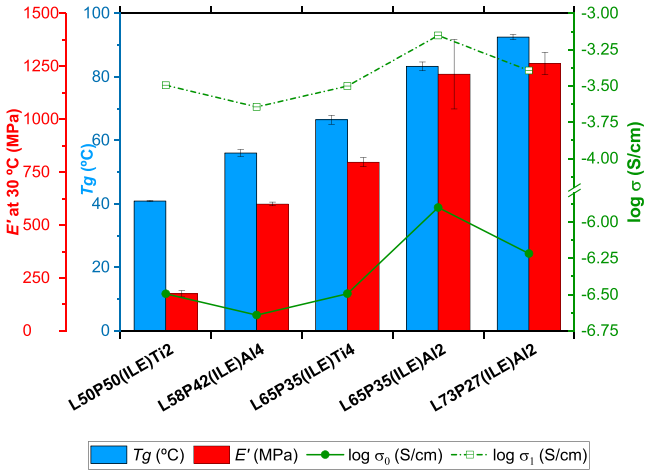

Figure 7. DMTA data and ionic conductivities of the samples L50P50(ILE)Ti2, L58P42(ILE)Al4, L65P35(ILE)Ti4, L65P35(ILE)-Al2, and L73P27(ILE)Al2.

data, the nanocomposite L65P35(ILE)Al2 exhibits the best combination of properties and, thus, can be considered a potential candidate as solid electrolyte for structural applications. The thermomechanical properties were T_g = 83 °C and E' at 30 °C = 1213 MPa, while the ionic conductivities were $\sigma_0 = 7 \times 10^{-4}$ S/cm and $\sigma_1 = 1.6 \times 10^{-6}$ S/cm.

In the bibliography, it is common to find multifunctionality plots for SPEs that indicate their comparison by plotting elastic modulus and ionic conductivity on a double logarithmic scale.[16,29,34] Figure 8 shows the comparison of the structural HEs of the state-of-the-art reported with HEs developed in this work. In the figure, a star indicates the ideal multifunctional HE, which would have the elastic modulus of an aeronautical epoxy resin (for example, Araldite LY556/XB3473 with E = 2.65 GPa) and the conductivity of ionic liquid EMITFSI ($\sigma = 7.8 \times 10^{-3}$ S/cm). Thus, electrolytes with properties closer to ideal indicate higher multifunctionality. Specifically, the square and triangular points correspond to the electrolytes of the state-of-the-art and spherical points refer to HEs developed in this work. Here, the elastic modulus was specified depending

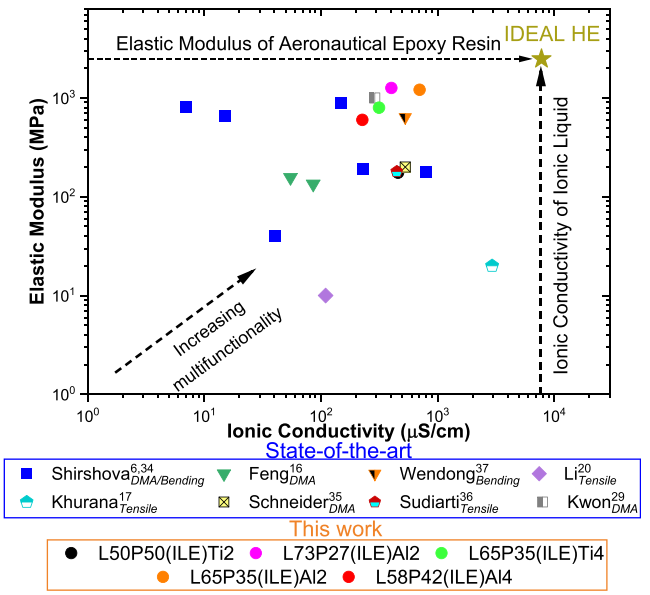

Figure 8. Summary of ionic conductivity and elastic modulus data on structural hybrid electrolytes. The superscript indicates the reference of each work, and the subscript shows the mechanical test that was carried out to establish the elastic modulus.

on the mechanical tests that were carried out in each work (DMTA, bending or tensile test).

In this regard, HEs developed in this work are in a privileged position with respect to the state-of-the-art, because its properties were closest to the ideal HE. Specifically, the multifunctionality of the L65P35(ILE)Al2 electrolyte stands out above those developed by the groups of Shirshova,[6,35] Schneider,[36] Sudiarti,[37] Kwon,[29] and Wendong,[38] which are structural electrolytes with high impact in the field.

Nevertheless, the multifunctionality denoted by Figure 8 is limited, since it does not consider the T_g of HEs, which is a determining property in structural polymers and, thus, in the multifunctionality. In this regard, the T_g of an aeronautical epoxy resin are around 150 °C. Therefore, the T_g values of Feng et al.'s[16] electrolytes are 43 and 46 °C, Shirshova et al.'s[6,35] electrolytes are around 60−65 °C, and Kwon et al.'s[29] electrolyte is 57 °C, that suppose lower values than the L65P35(ILE)Al2 reported in this work, that is 83 °C. The other works presented in Figure 8 did not report T_g values.

The thermomechanical properties and ionic conductivity of L65P35(ILE)Al2 nanocomposite are closer to the ideal multifunctional electrolyte with respect to the state-of-the-art. For this reason, it would be very promising as hybrid electrolyte in structural applications.

Effect of Alumina Nanoparticles in L65P35(ILE) Electrolyte: L65P35(ILE)Al2. The incorporation of alumina to the electrolyte L65P35(ILE) produces an important improvement in the thermomechanical properties and ionic conductivity, as has been reported in the previous sections. Therefore, in order to continue explaining in detail the influence of these nanoparticles, L65P35(ILE) and L65P35-(ILE)Al2 electrolytes were characterized by EIS at different temperatures, CVs, and LSVs.

The behavior of the ionic conductivity at different temperatures reveals information related to the ion transport mechanism. Thus, the EIS tests were carried out from 20 to 120 °C, taking a measurement every 10 °C. As it can be seen in

https://doi.org/10.1021/acsaem.1c03836
ACS Appl. Energy Mater. 2022, 5, 4247−4258

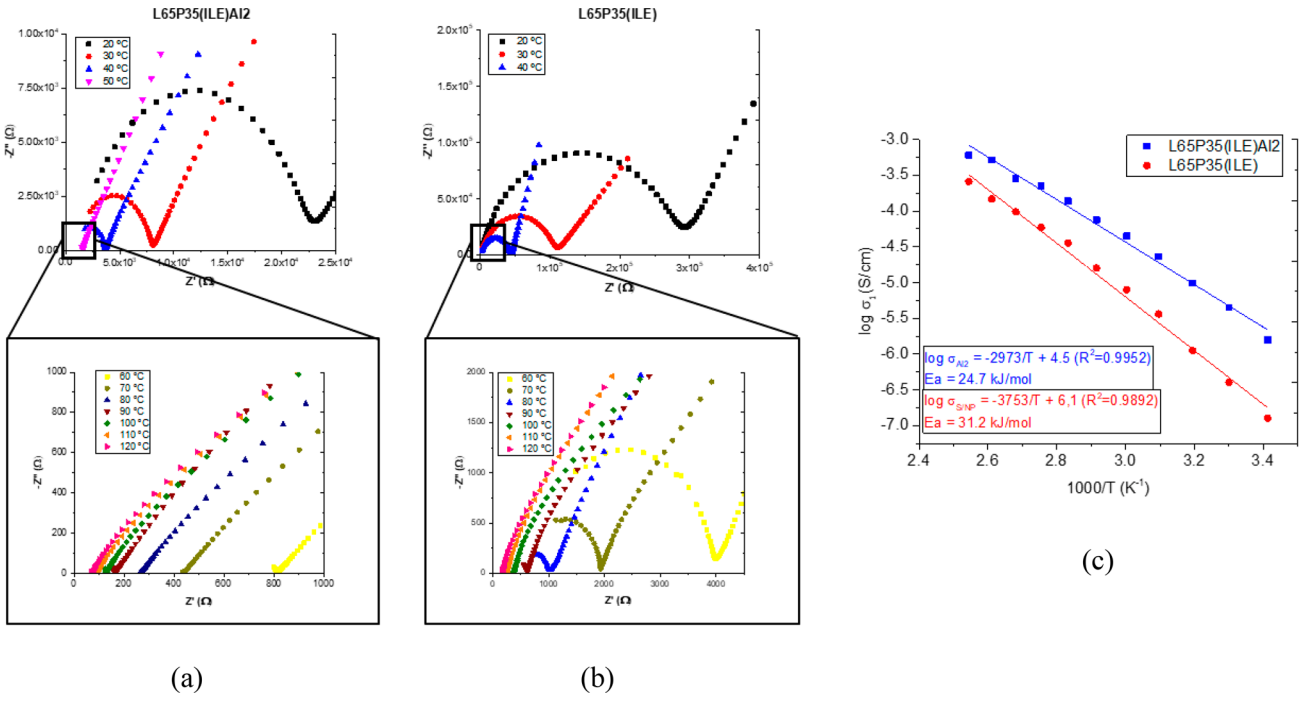

Figure 9. Nyquist plots of the samples (a) L65P35(ILE)Al2 and (b) L65P35(ILE) at different temperatures and (c) fit with the Arrhenius model for ionic transport.

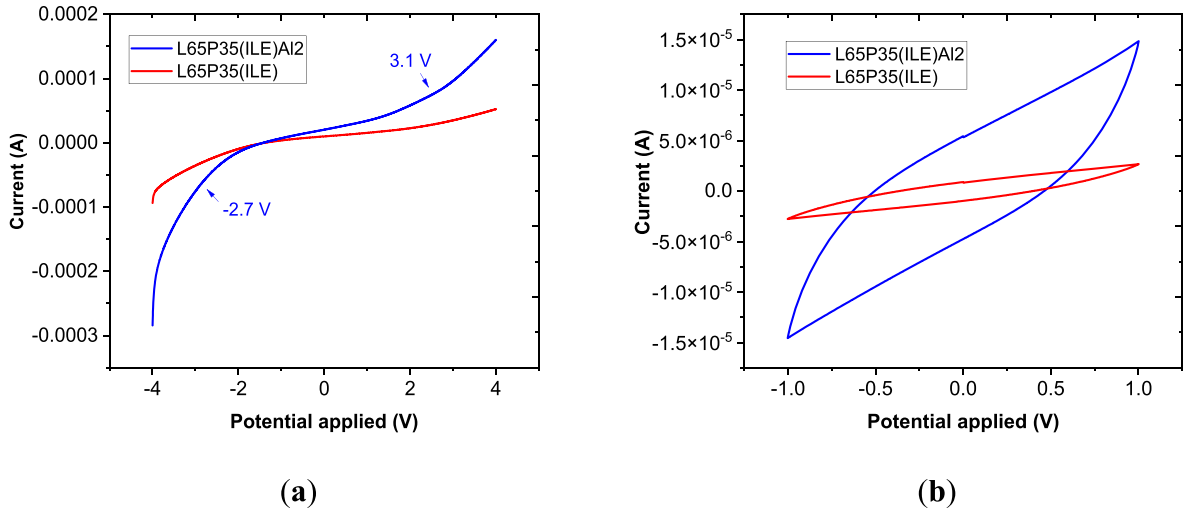

Figure 10. (a) Electrochemical stability window and (b) cyclic voltammetry of L65P35(ILE)Al2 and L65P35(ILE) electrolytes.

the Nyquist diagrams in Figure 9a,b, the ionic conductivity (σ_1) increased when test temperature increased, since a smaller size of the semicircle located at high frequencies is observed. The increase of temperature enhances ionic conductivity because ion diffusion mechanisms are favored, and the mobility of the polymer chains is accentuated. Among the existing ion transport models,[33] L65P35(ILE)Al2 and L65P35(ILE) electrolytes have followed Arrhenius model given by

$$\sigma_1 = \sigma_p \exp\left(-\frac{E_a}{k_B T}\right) \quad (2)$$

where σ_p, E_a, and k_B are the pre-exponential factor, activation energy and Boltzmann constant, respectively.

The electrolyte with alumina nanoparticles exhibited an E_a = 24.7 kJ/mol, and the electrolyte without alumina had an E_a = 31.2 kJ/mol. Again, these nanoparticles favor a structure that improves ion mobility due to the creation of cylindrical tunnels, previously explained. In this regard, both electrolytes had the same behavior regardless of the temperature, even above or below their T_g. These values are slightly higher than those obtained for DGEBA-based flexible composites containing at least 50% of ionic liquid or ionic species (some examples: Soares's electrolyte 10.3 kJ/mol,[39] Kwon's electrolyte 8.6 kJ/mol[29] for comparison), but lower compared to samples with similar content of the ionic species.[39,40]

An electrochemical stability window is an important parameter for the electrochemical performance of SPE, which it is determined by linear sweep voltammetry. Figure 10a shows the stability windows of L65P35(ILE)Al2 and L65P35(ILE) electrolytes. The electrolyte without alumina had a greater window of electrochemical stability than the

https://doi.org/10.1021/acsaem.1c03836
ACS Appl. Energy Mater. 2022, 5, 4247−4258

electrolyte with nanoparticles. This can be explained because the higher ionic mobility is usually manifested in lower electrochemical instability, between electrolytes with similar base material, that has been previously reported.[33] Moreover, the ionic liquid used in this study showed an electrochemical stability with anodic and cathodic limits of 1.54 and −2.76,[41] respectively, that is lower than the window reported in SPEs due to a lower free mobility of ions.[33,42,43]

To evaluate the effect of alumina on the capacitance, the samples were analyzed by cyclic voltammetry. The voltammograms obtained at room temperature for the potential window between −1 and 1 V are shown in Figure 10b. No significant distortions were noted in the shape of the curve for these electrolytes. This non-"duck" shape indicates that there are not redox reactions inside the material.[44]

From these curves, it was possible to calculate the specific capacitance, C_{spm} or C_{spa}, of the stainless-steel/HE/stainless-steel system by applying the following eq 3:

$$C_{sp} = \frac{1}{xv(V_c - V_a)} \int_{V_a}^{V_c} I \, dV \tag{3}$$

where x is the mass of the electrolyte (C_{spm}) or the area in contact with electrodes (C_{spa}), v the scan velocity rate, fixed at 0.1 V/s, and $V_c - V_a$ the voltage window, set at 2 V.

Table 3 summarizes the C_{sp} for these electrolytes in study. As expected, the electrolyte with nanoparticles (L65P35(ILE)-Al2) had a specific capacitance higher than the base electrolyte (L65P35(ILE)), specifically, about 6 times higher. This was explained by the higher ionic conductivity of L65P35(ILE)Al2 reported.

Table 3. Specific Capacitance (Mass or Area) of L65P35(ILE)Al2 and L65P35(ILE) Electrolytes

sample	C_{spm} (F/g)	C_{spa} (F/cm^2)
L65P35(ILE)Al2	5.6×10^{-5}	1.5×10^{-6}
L65P35(ILE)	9.7×10^{-6}	2.4×10^{-6}

In order to get some information about the way the alumina nanoparticles interact with the cross-linked matrix, the sample was analyzed by ^{13}C, ^{19}F, and ^{27}Al CP NMR. The ^{13}C spectrum (Figure S8) is consistent with a typical DGEBA/PEGDGE mixture of resins showing the signals corresponding to the CH_2-CH_2-O groups of the PEGDGE and aliphatic/aromatic carbons of DGEBA. The ^{19}F CP NMR spectrum (Figure S9) shows three signals, one sharp narrow peak at −79.45 ppm attributed to a fast-speed mobile species (free TFSI$^-$) and two more broad peaks at 77.16 and −79.06 ppm that can be attributed to a more hindered species (TFSI$^-$) present in two different chemical environments.

The ^{27}Al CP NMR (shown in Figure 11) shows two main signals at 8.97 and 64.32 ppm, the typical signals for octahedral and tetrahedral aluminum atoms in γ-Al_2O_3. Two satellites can also be observed at 151.17 and −116.32 ppm.

The alumina used in this study is slightly acidic, so it was possible that the predominant mechanism in ionic conductivity would be through Lewis acid interactions as proposed by Croce et al.[22] Specifically, acidic and neutral Al_2O_3 form hydrogen bonds with anions (TFSI$^-$) and with oxygens in ethylene oxide chains (PEGDGE), promoting the ionic liquid dissociation and weakening cation−polymer coordination (Figure 12).

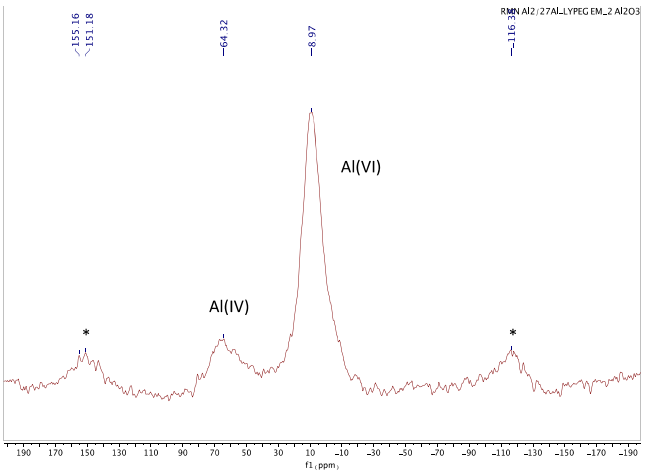

Figure 11. ^{27}Al CP NMR spectrum of sample L65P35(ILE)Al2 at room temperature.

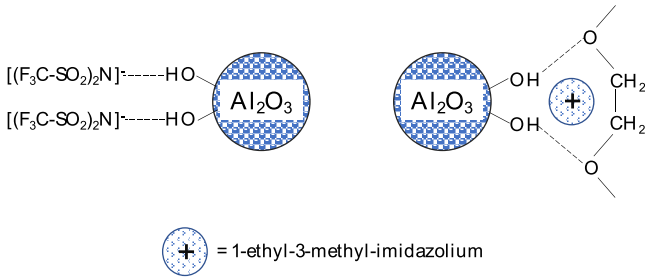

Figure 12. Lewis acid interactions of alumina and a salt.

It has also been proposed that the alumina does not interact directly with the polymeric chains and the improvement of the ionic conductivity was attributed to Lewis acid−base type surface interactions of ionic species with O/OH groups on the filler surface.[23]

According to the ^{27}Al CP NMR analyses, the aluminum atoms were mainly incorporated in an octahedral environment probably surrounded by the oxygen atoms (ethylene oxide units) of PEGDGE. The acidic alumina interacts with the oxygen atoms of the matrix and with the TFSI$^-$. Because the ^{19}F CP NMR spectrum shows three signals for the CF_3 groups of the anion (TFSI$^-$), we can propose that one of the broader peaks previously attributed to a more-hindered species can correspond to the anion close to the nanoparticle surface. The other broader signal, as it has been previously observed for similar samples,[5] can be assigned to the TFSI$^-$ anions in the salt, which means associated with the cation.

CONCLUSIONS

The thermomechanical and electrochemical properties of solid polymer electrolytes based on a blend of epoxy resins (L and P), 1-ethyl-3-methylimidazolium bis(trifluoromethylsulfonyl)-imide ionic liquid and titania (<25 nm) or alumina (<13 nm) nanoparticles were investigated. The correct combination of these components represented a good example of how a solid polymer electrolyte could be tuned and optimized.

In general, the incorporation of low percentages of ceramic nanoparticles (around 2 wt %) to the base electrolyte represented an improvement of the thermomechanical properties and ionic conductivity due to the well-dispersed nanoparticles in the matrix. By contrast, high percentages of

https://doi.org/10.1021/acsaem.1c03836
ACS Appl. Energy Mater. 2022, 5, 4247−4258

nanoparticles reduced these properties because agglomerates of nanoparticles appeared. Moreover, alumina tended to show better properties due to its smaller size, in comparison with titania.

The optimized electrolyte L65P35(ILE)Al2 showed thermomechanical properties of T_g = 83 °C and E' at 30 °C = 1.2 GPa, while the ionic conductivities were $\sigma_0 = 7 \times 10^{-4}$ S/cm and $\sigma_1 = 1.6 \times 10^{-6}$ S/cm. This electrolyte followed the Arrhenius ion transport model (E_a = 24.7 kJ/mol) and a cyclic voltammetry test showed $C_{spm} = 5.6 \times \cdot 10^{-5}$ F/g and $C_{spa} = 1.5 \times 10^{-6}$ F/cm^2, values significantly better than the base electrolyte without alumina L65P35(ILE). Furthermore, the acidic alumina used in this study promoted Lewis acid interactions as the predominant mechanism in ionic conductivity. These results proved that L65P35(ILE)Al2 nanocomposite reaches properties closer to the ideal multifunctional electrolyte (thermomechanical behavior of aeronautical epoxy resin and conductivity of an ionic liquid) than those developed in the state-of-the-art. Thus, electrolyte would be very promising as hybrid electrolyte in structural applications.

■ ASSOCIATED CONTENT

Supporting Information

The Supporting Information is available free of charge at https://pubs.acs.org/doi/10.1021/acsaem.1c03836.

Nyquist plots, equivalent circuit parameters, and CP-MAS NMR spectra for different electrolytes (PDF)

■ AUTHOR INFORMATION

Corresponding Author

Antonio del Bosque − *Materials Science and Engineering Area, Escuela Superior de Ciencias Experimentales y Tecnología, Universidad Rey Juan Carlos, Madrid 28933, Spain;* orcid.org/0000-0002-8301-2159; Phone: +34 914 88 46 21; Email: antonio.delbosque@urjc.es

Authors

Bianca K. Muñoz − *Materials Science and Engineering Area, Escuela Superior de Ciencias Experimentales y Tecnología, Universidad Rey Juan Carlos, Madrid 28933, Spain*

María Sánchez − *Materials Science and Engineering Area, Escuela Superior de Ciencias Experimentales y Tecnología, Universidad Rey Juan Carlos, Madrid 28933, Spain*

Alejandro Ureña − *Materials Science and Engineering Area, Escuela Superior de Ciencias Experimentales y Tecnología, Universidad Rey Juan Carlos, Madrid 28933, Spain*

Complete contact information is available at: https://pubs.acs.org/10.1021/acsaem.1c03836

Notes

The authors declare no competing financial interest.

■ ACKNOWLEDGMENTS

This research was funded by the Agencia Estatal de Investigación of Spanish Government [Project MULTIFUNC-EVs PID2019-107874RB-I00] and Comunidad de Madrid Government [Project ADITIMAT-CM (S2018/NMT-4411)].

■ REFERENCES

(1) Shaikh, M. S.; Shaikh, P. H.; Qureshi, K.; Bhatti, I. Green House Effect and Carbon Foot Print. In *Encyclopedia of Renewable and Sustainable Materials*; Elsevier, 2018; pp 120−125. DOI: 10.1016/b978-0-12-803581-8.10456-4.

(2) Asp, L. E.; Greenhalgh, E. S. Multifunctional Structural Battery and Supercapacitor Composites. In *Multifunctionality of Polymer Composites: Challenges and New Solutions*; Elsevier Inc., 2015; pp 619−661. DOI: 10.1016/B978-0-323-26434-1.00020-9.

(3) Chan, K. Y.; Jia, B.; Lin, H.; Hameed, N.; Lee, J. H.; Lau, K. T. A Critical Review on Multifunctional Composites as Structural Capacitors for Energy Storage. In *Composite Structures*; Elsevier, 2018; pp 126−142. DOI: 10.1016/j.compstruct.2017.12.072.

(4) Xu, Y.; Lu, W.; Xu, G.; Chou, T. W. Structural Supercapacitor Composites: A Review. *Compos. Sci. Technol.* **2021**, *204*, 108636.

(5) Muñoz, B. K.; del Bosque, A.; Sánchez, M.; Utrilla, V.; Prolongo, S. G.; Prolongo, M. G.; Ureña, A. Epoxy Resin Systems Modified with Ionic Liquids and Ceramic Nanoparticles as Structural Composites for Multifunctional Applications. *Polymer (Guildf).* **2021**, *214*, 123233.

(6) Shirshova, N.; Qian, H.; Shaffer, M. S. P.; Steinke, J. H. G.; Greenhalgh, E. S.; Curtis, P. T.; Kucernak, A.; Bismarck, A. Structural Composite Supercapacitors. *Compos. Part A Appl. Sci. Manuf.* **2013**, *46*, 96−107.

(7) Liu, X.; Li, X.; Li, H.; Wu, H. Bin. Recent Progress of Hybrid Solid-State Electrolytes for Lithium Batteries. *Chem. - A Eur. J.* **2018**, *24* (69), 18293−18306.

(8) Liang, J.; Luo, J.; Sun, Q.; Yang, X.; Li, R.; Sun, X. Recent Progress on Solid-State Hybrid Electrolytes for Solid-State Lithium Batteries. *Energy Storage Mater.* **2019**, *21*, 308−334.

(9) Yang, G.; Song, Y.; Wang, Q.; Zhang, L.; Deng, L. Review of Ionic Liquids Containing, Polymer/Inorganic Hybrid Electrolytes for Lithium Metal Batteries. *Mater. Des.* **2020**, *190*, 108563.

(10) Guo, Q.; Han, Y.; Wang, H.; Xiong, S.; Sun, W.; Zheng, C.; Xie, K. Flame Retardant and Stable Li1.5Al0.5Ge1.5(PO4)3-Supported Ionic Liquid Gel Polymer Electrolytes for High Safety Rechargeable Solid-State Lithium Metal Batteries. *J. Phys. Chem. C* **2018**, *122* (19), 10334−10342.

(11) Austin Suthanthiraraj, S.; Johnsi, M. Nanocomposite Polymer Electrolytes. *Ionics* **2017**, *23*, 2531−2542.

(12) Pryamitsyn, V.; Ganesan, V. Interplay between Depletion and Electrostatic Interactions in Polyelectrolyte-Nanoparticle Systems. *Macromolecules* **2014**, *47* (17), 6095−6112.

(13) Chung, S. H.; Wang, Y.; Persi, L.; Croce, F.; Greenbaum, S. G.; Scrosati, B.; Plichta, E. Enhancement of Ion Transport in Polymer Electrolytes by Addition of Nanoscale Inorganic Oxides. *J. Power Sources* **2001**, *97*−*98*, 644−648.

(14) Yuuki, T.; Konosu, Y.; Ashizawa, M.; Iwahashi, T.; Ouchi, Y.; Tominaga, Y.; Ooyabu, R.; Matsumoto, H.; Matsumoto, H. Ionic Liquid-Based Electrolytes Containing Surface-Functionalized Inorganic Nanofibers for Quasisolid Lithium Batteries. *ACS Omega* **2017**, *2* (3), 835−841.

(15) Chaurasia, S. K.; Chandra, A. Organic-Inorganic Hybrid Electrolytes by in-Situ Dispersion of Silica Nanospheres in Polymer Matrix. *Solid State Ionics* **2017**, *307*, 35−43.

(16) Feng, Q.; Yang, J.; Yu, Y.; Tian, F.; Zhang, B.; Feng, M.; Wang, S. The Ionic Conductivity, Mechanical Performance and Morphology of Two-Phase Structural Electrolytes Based on Polyethylene Glycol, Epoxy Resin and Nano-Silica. *Mater. Sci. Eng., B* **2017**, *219*, 37−44.

(17) Khurana, S.; Negi, S.; Chandra, A. Effect of Surface Modification of Dispersoid on Hybrid Polymer Electrolyte. *Polym. Test.* **2021**, *96*, 107118.

(18) Chen, N.; Xing, Y.; Wang, L.; Liu, F.; Li, L.; Chen, R.; Wu, F.; Guo, S. Tai Chi" Philosophy Driven Rigid-Flexible Hybrid Ionogel Electrolyte for High-Performance Lithium Battery. *Nano Energy* **2018**, *47*, 35−42.

(19) Pignanelli, F.; Romero, M.; Castiglioni, J.; Faccio, R.; Mombrú, A. W. Novel Synergistic in Situ Synthesis of Lithium-Ion Poly-(Ethylene Citrate)-TiO2 Nanocomposites as Promising Fluorine-Free Solid Polymer Electrolytes for Lithium Batteries. *J. Phys. Chem. Solids* **2019**, *135*, 109082.

(20) Li, S.; Jiang, H.; Tang, T.; Nie, Y.; Zhang, Z.; Zhou, Q. Improved Electrochemical and Mechanical Performance of Epoxy-Based Electrolytes Doped with Mesoporous TiO2. *Mater. Chem. Phys.* **2018**, *205*, 23−28.
(21) Sánchez-Romate, X. F.; Bosque, A. D.; Artigas-Arnaudas, J.; Muñoz, B. K.; Sánchez, M.; Ureña, A. A Proof of Concept of a Structural Supercapacitor Made of Graphene Coated Woven Carbon Fibers: EIS Study and Mechanical Performance. *Electrochim. Acta* **2021**, *370*, 137746.
(22) Croce, F.; Persi, L.; Scrosati, B.; Serraino-Fiory, F.; Plichta, E.; Hendrickson, M. A. Role of the Ceramic Fillers in Enhancing the Transport Properties of Composite Polymer Electrolytes. *Electrochim. Acta* **2001**, *46* (16), 2457−2461.
(23) Dissanayake, M. A. K. L.; Jayathilaka, P. A. R. D.; Bokalawala, R. S. P.; Albinsson, I.; Mellander, B.-E. Effect of Concentration and Grain Size of Alumina Filler on the Ionic Conductivity Enhancement of the (PEO)9LiCF3SO3:Al2O3 Composite Polymer Electrolyte. *J. Power Sources* **2003**, *119*−*121*, 409−414.
(24) Marcinek, M.; Bac, A.; Lipka, P.; Zalewska, A.; Żukowska, G.; Borkowska, R.; Wieczorek, W. Effect of Filler Surface Group on Ionic Interactions in PEG-LiClO4-Al2O3 Composite Polyether Electrolytes. *J. Phys. Chem. B* **2000**, *104* (47), 11088−11093.
(25) Best, A. S.; Adebahr, J.; Jacobsson, P.; MacFarlane, D. R.; Forsyth, M. Microscopic Interactions in Nanocomposite Electrolytes. *Macromolecules* **2001**, *34* (13), 4549−4555.
(26) Singh, S.; Rafiuddin. Rafiuddin. Preparation, Characterization and Electrical Studies of Polymer Composite Solid Electrolyte (1−x) Polyaniline-Ag_3PO_4·xAl_2O_3. *Mater. Today: Proc.* **2020**, *29*, 363−371.
(27) Kumar, M. S.; Rao, M. C. Effect of Al2O3 on Structural and Dielectric Properties of PVP-CH3COONa Based Solid Polymer Electrolyte Films for Energy Storage Devices. *Heliyon* **2019**, *5* (10), e02727.
(28) Pradeepa, P.; Sowmya, G.; Edwinraj, S.; Fareetha Begum, G.; Ramesh Prabhu, M. Influence of Al_2O_3 on the Structure and Electrochemical Properties of PVAc/PMMA Based Blend Composite Polymer Electrolytes. *Mater. Today: Proc.* **2016**, *3*, 2187−2196.
(29) Kwon, S. J.; Kim, T.; Jung, B. M.; Lee, S. B.; Choi, U. H. Multifunctional Epoxy-Based Solid Polymer Electrolytes for Solid-State Supercapacitors. *ACS Appl. Mater. Interfaces* **2018**, *10* (41), 35108−35117.
(30) Muñoz, B. K.; del Bosque, A.; Sánchez, M.; Utrilla, V.; Prolongo, S. G.; Prolongo, M. G.; Ureña, A. Epoxy Resin Systems Modified with Ionic Liquids and Ceramic Nanoparticles as Structural Composites for Multifunctional Applications. *Polymer (Guildf).* **2021**, *214*, 123233.
(31) Lorero, I.; Campo, M.; Del Rosario, G.; López, F. A.; Prolongo, S. G. New Manufacturing Process of Composites Reinforced with ZnO Nanoparticles Recycled from Alkaline Batteries. *Polymers* **2020**, *12* (7), 1619.
(32) Hanemann, T. Influence of Particle Properties on the Viscosity of Polymer-Alumina Composites. *Ceram. Int.* **2008**, *34* (8), 2099−2105.
(33) Aziz, S. B.; Woo, T. J.; Kadir, M. F. Z.; Ahmed, H. M. A Conceptual Review on Polymer Electrolytes and Ion Transport Models. *J. Sci. Adv. Mater. Devices* **2018**, *3* (1), 1−17.
(34) Yu, A.; Chabot, V.; Zhang, J. *Electrochemical Supercapacitors for Energy Storage and Delivery: Fundamentals and Applications*; CRC Press, 2017. DOI: 10.1201/b14671.
(35) Shirshova, N.; Bismarck, A.; Greenhalgh, E. S.; Johansson, P.; Kalinka, G.; Marczewski, M. J.; Shaffer, M. S. P.; Wienrich, M. Composition as a Means To Control Morphology and Properties of Epoxy Based Dual-Phase Structural Electrolytes. *J. Phys. Chem. C* **2014**, *118* (49), 28377−28387.
(36) Schneider, L. M.; Ihrner, N.; Zenkert, D.; Johansson, M. Bicontinuous Electrolytes via Thermally Initiated Polymerization for Structural Lithium Ion Batteries. *ACS Appl. Energy Mater.* **2019**, *2* (6), 4362−4369.
(37) Sudiarti, T.; Wahyuningrum, D.; Bundjali, B.; Made Arcana, I. Mechanical Strength and Ionic Conductivity of Polymer Electrolyte Membranes Prepared from Cellulose Acetate-Lithium Perchlorate. *IOP Conf. Ser. Mater. Sci. Eng.* **2017**, *223*, 012052.
(38) Wendong, Q.; Dent, J.; Arrighi, V.; Cavalcanti, L.; Shaffer, M. S. P.; Shirshova, N. Biphasic Epoxy-Ionic Liquid Structural Electrolytes: Minimising Feature Size through Cure Cycle and Multifunctional Block-Copolymer Addition. *Multifunct. Mater.* **2021**, *4* (3), 035003.
(39) Oliveira da Silva, L. C.; Soares, B. New All Solid-State Polymer Electrolyte Based on Epoxy Resin and Ionic Liquid for High Temperature Applications. *J. Appl. Polym. Sci.* **2018**, *135*, 45838.
(40) Maksym, P.; Tarnacka, M.; Dzienia, A.; Matuszek, K.; Chrobok, A.; Kaminski, K.; Paluch, M. Enhanced Polymerization Rate and Conductivity of Ionic Liquid-Based Epoxy Resin. *Macromolecules* **2017**, *50* (8), 3262−3272.
(41) Klein, J. M.; Panichi, E.; Gurkan, B. Potential Dependent Capacitance of [EMIM][TFSI], [N1114][TFSI] and [PYR13][TFSI] Ionic Liquids on Glassy Carbon. *Phys. Chem. Chem. Phys.* **2019**, *21* (7), 3712−3720.
(42) Mohapatra, S. R.; Thakur, A. K.; Choudhary, R. N. P. Effect of Nanoscopic Confinement on Improvement in Ion Conduction and Stability Properties of an Intercalated Polymer Nanocomposite Electrolyte for Energy Storage Applications. *J. Power Sources* **2009**, *191* (2), 601−613.
(43) Dinoto, V.; Negro, E.; Lavina, S.; Vittadello, M. Hybrid Inorganic-Organic Polymer Electrolytes. *Polym. Electrolytes Fundam. Appl.* **2010**, 219−277.
(44) Elgrishi, N.; Rountree, K. J.; McCarthy, B. D.; Rountree, E. S.; Eisenhart, T. T.; Dempsey, J. L. A Practical Beginner's Guide to Cyclic Voltammetry. *J. Chem. Educ.* **2018**, *95* (2), 197−206.